Journal of Luminescence 132 (2012) 1584–1588

Contents lists available at SciVerse ScienceDirect

Journal of Luminescence

journal homepage: www.elsevier.com/locate/jlumin

Electronic band structure of GaAs/$Al_xGa_{1-x}As$ superlattice in an intense laser field

S. Sakiroglu [a,*], U. Yesilgul [b], F. Ungan [b], C.A. Duque [c], E. Kasapoglu [b], H. Sari [b], I. Sokmen [a]

[a] Physics Department, Faculty of Science, Dokuz Eylül University, 35160 İzmir, Turkey
[b] Physics Department, Faculty of Science, Cumhuriyet University, 58140 Sivas, Turkey
[c] Instituto de Física, Universidad de Antioquia, AA 1226, Medellín, Colombia

ARTICLE INFO

Article history:
Received 10 October 2011
Received in revised form
12 January 2012
Accepted 30 January 2012
Available online 7 February 2012

Keywords:
Superlattices
Intense laser fields
Laser-dressed potential

ABSTRACT

We perform theoretical calculations for the band structure of semiconductor superlattice under intense high-frequency laser field. In the frame of the non-perturbative approach, the laser effects are included via laser-dressed potential. Results reveal that an intense laser field creates an additional geometric confinement on the electronic states. Numerical results show that when tuning the strength of the laser field significant changes come in the electronic energy levels and density of states.

1. Introduction

Technological developments in the growth techniques in recent years made possible the fabrication of low-dimensional nanostructures such as single and multiple quantum wells, quantum dots, quantum wires and superlattices [1]. Because of their intrinsic physical properties and their technological applications in electronic and optoelectronic devices [2], there has been an increasing interest on semiconductor nanostructures [3,4]. In addition to this, advances of high-power, long-wavelength, linearly polarized laser sources has opened a new possibility in the use of lasers as a tool to manipulate electronic wavefunctions [5–7]. Some interesting phenomena associated with the external field arise in case of system with reduced dimensionality owing to the confinement of the charge carriers. Application of an intense laser-field (ILF) radiation considerably affects the electrical and optical properties of low-dimensional semiconducting structures [8–13].

Semiconductor superlattice (SSL) is based on a periodic structure of alternating layers of two semiconductor materials of almost equal lattice constant with wide and narrow band gaps [14,15]. The artificial periodicity of the SSL perturbs the band structure of the underlying materials to produce new (miniband) conduction states, the energies of which can be selectively tuned through the design of the SSL [16]. Localization of the electronic states in the material is highly sensitive to the barrier width and height, impurity distribution, effective mass, and the action of external fields [17]. The typical energy scales in superlattices or multiple quantum wells, such as miniband width, exciton level spacing, Bloch oscillation frequency, etc., are in the terahertz (THz) regime [18]. Therefore, these structures can be served as a tool to investigate the effects of an ILF. Understanding the basic physics involved in the external field-semiconductor interaction may assist in designing optoelectronic devices with high frequency. Recent experiments on the optical properties of SSLs irradiated by an intense THz radiation revealed some interesting phenomena, including the dynamical Franz-Keldysh effect, the ac Stark effect, the dynamical localization, and the inverse Bloch oscillations [19,18]. Many theoretical efforts have been devoted to the realization of phenomena of the irradiated SSLs, most notably in their transport properties where many nonlinear processes arise out [20]. Holthaus [21,22] investigated the quantum mechanics of laser-driven superlattice and showed the controllability of the quasienergy miniband by the strength and the frequency of the driving far-infrared laser radiation. Analysis of the conditions under which collapse of magnetic subbands and suppression on N-photon absorption or emission precesses occur has been considered by Rodriguez-Castellenos et al. [19]. Yun and coworkers [18] studied the excitonic optical absorption and discussed the interplay between the dynamical localization and the ac Stark effect. It is well known that significant modifications in the shape of the confining potential of the quantum well emerge in a high-frequency ILF [23–25]. Although the main physics for quantum well structures in high-frequency laser field

* Corresponding author. Tel.: +90 232 301 86 61; fax: +90 232 453 41 88.
E-mail address: serpil.sakiroglu@deu.edu.tr (S. Sakiroglu).

0022-2313/$ - see front matter © 2012 Elsevier B.V. All rights reserved.
doi:10.1016/j.jlumin.2012.01.060

is generally clear, many details on SSLs have not yet been explored. So far, to our knowledge, the consequences of subjecting the charge carriers to an ILF and treating the problem in the frame of "laser-dressed potential" has not been yet investigated.

The purpose of the present paper is a theoretical study of the influence of an intense, linearly polarized, non-resonant laser radiation on the potential profile, the electronic band structure and the density of states (DOS) of GaAs/$Al_xGa_{1-x}As$ superlattices. The investigations are based upon a non-perturbative theory that has been developed to describe the atomic behavior in intense high-frequency laser fields. The effect of the radiation is expressed in the "dressed" potential which renormalizes electronic bands. Calculations on the electronic structure of the system as a function of the laser-dressing parameter has been carried out.

This paper is organized as follows. In Section 2 overview of the Kronig-Penney formalism for GaAs/$Al_xGa_{1-x}As$ SSL and then the calculation model used to describe the laser-dressed SSL for the formation of electronic energy bands is discussed. Numerical results for the electronic energies versus the laser-dressing parameter are presented in Section 3. Finally, Section 4 is dedicated to the conclusions.

2. Theory and formalism

The one-dimensional Kronig-Penney (KP) model consists of an infinite series of rectangular barriers with potential height V_0 and width L_b, separated by wells of width L_w resulting in a periodic potential with period $L=L_w+L_b$ [26]. As well known solution of the Schrödinger equation for an electron in this periodic potential introduces the formation of electronic energy bands as well as energy band gaps. In case of a variable charge carrier effective masses, m_w^* and m_b^* in the well and barrier, respectively, the solution of the Schrödinger equation can be obtained by using the basis of envelope-function approximation. The Schrödinger equation then is written as

$$\left[-\frac{\hbar^2}{2}\frac{d}{dz}\left(\frac{1}{m^*(z)}\frac{d}{dz}\right)+V(z)\right]\varphi(z)=E\varphi(z), \tag{1}$$

where the periodic potential of the superlattice satisfies the following translational invariance $V(z+L)=V(z)$ and discontinuity at the interfaces of the two kinds of materials with the local masses $m^*(z)$,

$$V(z)=\begin{cases} V_0, \\ 0; \end{cases} \qquad m^*(z)=\begin{cases} m_b^*, & -L_b<z<0, \\ m_w^*, & 0<z<L_w. \end{cases} \tag{2}$$

The solution of the Schrödinger's equation for the KP potential is obtained by assuming the Bloch periodicity condition

$$\varphi(z+L)=\exp(ik_zL)\varphi(z), \tag{3}$$

where k_z is the wavevector with the manifold of $-\pi/L<k_z<\pi/L$. The KP model assumes that the electron wave function and its weighted derivative are continuous at the interface of quantum well and potential barrier [27]. Then the solution of the Schrödinger equation in Eq. (1) is obtained from the determinant of a 4×4 matrix resulting from four boundary conditions. By the definitions $k_w=\sqrt{2m_w^*E/\hbar^2}$, $k_b=\sqrt{2m_b^*(E-V_0)/\hbar^2}\geq0$, and $\kappa_b=\sqrt{2m_b^*(V_0-E)/\hbar^2}\geq0$, in case $E\geq V_0$, the solution of this determinant is

$$\cos(k_zL)=\cos(k_wL_w)\cos(k_bL_b) -\frac{1}{2}\left(\frac{m_b^*k_w}{m_w^*k_b}+\frac{m_w^*k_b}{m_b^*k_w}\right)\sin(k_wL_w)\sin(k_bL_b)$$

and, other case $V_0\geq E$, the solution is

$$\cos(k_zL)=\cos(k_wL_w)\cosh(\kappa_bL_b) -\frac{1}{2}\left(\frac{m_b^*k_w}{m_w^*\kappa_b}-\frac{m_w^*\kappa_b}{m_b^*k_w}\right)\sin(k_wL_w)\sinh(\kappa_bL_b)$$

in the form.

The method of approach used in the present calculation is based on a non-perturbative theory describing the atomic behavior in intense high-frequency laser fields [28]. Non-resonant electromagnetic (EM) radiation is assumed to be a linearly polarized along the growth axis of a structure and it is represented by a monochromatic plane wave with a frequency ω. Determination of the electronic states implies the inclusion of the potential corresponding to the radiation field to the kinetic part of the Hamiltonian. This problem can be handled semiclassically by combining a quantum description of the particle with a classical description of the radiation field [29].

For a slowly varying field in the physically important region of the space, upon the non-relativistic dipole approximation the vector potential of the EM field can be expressed as $\mathbf{A}(r,t)\approx\mathbf{A}(t)$. For any oscillatory $\mathbf{A}(t)$, the Kramers–Henneberger (KH) unitary translational transformation [30] can be applied in order to transfer the time dependence from the kinetic to the potential term in the Hamiltonian. This transformation leads to time-dependent Schrödinger equation given as

$$-\frac{\hbar^2}{2m^*}\nabla^2\Psi(\vec{r},t)+V(\vec{r}+\vec{\alpha}(t))\Psi(\vec{r},t)=i\hbar\frac{\partial\Psi(\vec{r},t)}{\partial t}. \tag{4}$$

Here $V(\vec{r})$ is the atomic potential and $\alpha(t)=e/m^*\int^t A(t')\,dt'$ [31]. For a monochromatic laser field with a strength of F_0, the vector potential is assumed to be $\mathbf{A}(t)=A_0\cos(\omega t)\hat{z}$ where $A_0=F_0/\omega$ and $\hat{z}$ is the unity vector for the z-axis direction chosen to be a growth direction of the SSL. Then we have $\alpha(t)=\alpha_0\sin(\omega t)$, where $\alpha_0\equiv eA_0/m^*\omega$ is defined as a *laser dressing parameter*. The Eq. (4) emphasizes the fact that the electron motion in an EM field can be alternatively described in an accelerated frame that oscillates in the phase of the field [29]. Expansion of the oscillating potential $V(\vec{r}+\vec{\alpha}(t))$ in a Fourier–Floquet series in the case of a sufficiently high frequencies, bring out the dominating zeroth-order term which corresponds to the time average $1/T\int_0^T V(\vec{r}+\vec{\alpha}(t))\,dt$ $(T=2\pi/\omega)$ being the period of the radiation) [32–34], and called as a *laser-dressed* potential [29].Then electronic states of the system can be obtained via the solution of the following time-independent Schrödinger equation:

$$\left[-\frac{\hbar^2}{2}\frac{d}{dz}\left(\frac{1}{m^*(z)}\frac{d}{dz}\right)+\langle V(z,\alpha_0)\rangle\right]\varphi(z)=E\varphi(z), \tag{5}$$

where E is the energy level of zero-th Floquet component $\varphi(z)$ under ILF conditions.

In searching for an analytical expression for the laser dressed potential, after making the substitution $u=\omega t$, time-averaging integral is written as a sum of four integrals corresponding to the equally spaced subintervals of the integration domain. Extended details can be find in the reference [29]. Then the laser-dressed potential takes the form

$$\langle V(z,\alpha_0)\rangle=\frac{1}{\pi}\int_{-\alpha_0}^{+\alpha_0}\frac{d\alpha}{\sqrt{\alpha_0^2-\alpha^2}}V(z+\alpha). \tag{6}$$

It should be noticed that the approach of the laser-dressed potential is valid for a high-frequency regime, e.g., $\omega\tau\gg1$, where τ is the transition time of the electron. This condition is well satisfied in case of GaAs/$Al_xGa_{1-x}As$ quantum well of width 100 Å and with $x=0.3$ subjected to a monochromatic CO_2 laser beam of frequency ≈100 THz [35].

The conduction band superlattice potential with a period $L=L_w+L_b$ consists of GaAs of width L_w which serves as a well and $Al_xGa_{1-x}As$ of width L_b which serves as a barrier. In order to take quantum interference effects due to the superlattice potential, $V(z)$ is decomposed in a Fourier expansion of a general form

$$V(z)=\sum_{n=-\infty}^{+\infty} v_n\, e^{i(2\pi n/L)z}, \tag{7}$$

with expansion coefficients v_n given as

$$v_n=\frac{iV_0}{2\pi n}(1-e^{(i2\pi n/L)L_b}) \quad \text{and} \quad v_0=V_0\frac{L_b}{L}. \tag{8}$$

The laser-dressed potential corresponding to the superlattice potential in Eq. (7) is obtained by performing the time-averaging procedure presented in Eq. (6) and using Jacobi–Anger expansion [36] for the exponential term in the Fourier expansion of superlattice potential. Then we have

$$\langle V(z,\alpha_0)\rangle=\sum_{n=-\infty}^{+\infty} v_n\, e^{i(2\pi n/L)z}J_0\left(\frac{2\pi n}{L}\alpha_0\right). \tag{9}$$

Here $J_0(x)$ is zero-order Bessel function [37]. To obtain the laser-dressed eigenfunctions and eigenenergies associated with the SSL, the Hamiltonian in Eq. (5) is diagonalized in the model space spanned by using the time-independent wave function $\varphi(z)$

$$\varphi(z)=e^{ik_zz}\chi_{k_z}(z), \tag{10}$$

with

$$\chi_{k_z}(z)=\sum_{n=-(N-1)}^{+N} d_n^{k_z}\frac{e^{in(2\pi/L)z}}{\sqrt{L}}, \tag{11}$$

where $d_n^{k_z}$ are k_z-dependent unknown expansion coefficients for the periodic function $\chi_{k_z}(z)$. By applying the appropriate boundary continuity conditions at the interface between materials, the sum is extended over the number n which denote the number of sites in the unit cell, with length $L=2Nh$ and equally spaced size h. Eigenenergies with satisfying sufficient accuracy have been obtained for $N\geq 50$.

The density of states reflects the maximum number of carriers that occupy states with energies between E and $E+dE$. We start from the general expression of the local density of states in one dimension, assuming a quantum-numbers set $\alpha=\{n,k_z\}$ and spin degeneracy $g_s=2$, defined as

$$D(E,z)=g_s\sum_{n,k_z}\delta(E-E_n(k_z))\left|\varphi_{n,k_z}(z)\right|^2. \tag{12}$$

Here n is the band index, $E_n(k_z)$ is the band energy and $\varphi_{n,k_z}(z)$ is the solution of Eq. (5). By applying the scaling transformations such as $E\rightarrow E_h^*E$, $L\rightarrow a_0^*L$, and $k_z\rightarrow k_z/a_0^*$ where $a_0^*=4\pi\varepsilon\hbar^2/(m_w^*e^2)$ is the effective Bohr radius and $E_h^*=\hbar^2/(m_w^*a_0^{*2})$ is the effective Hartree energy, the integrated density of states is obtained as

$$D(E)=\frac{1}{2\pi}\frac{g_s}{E_h^*a_0^*}\sum_{n=1}^{\infty}\int_{-\pi/L}^{\pi/L}dk_z\delta(E-E_n(k_z)). \tag{13}$$

With the definitions, $D_0=m_w^*/(\pi\hbar^2)$ which is DOS of the two-dimensional free electron gas and λ defined to be the number of roots for the equation $E-E_n(k_{z,i})=0$, with $i=1,2,\ldots,\lambda$, the final expression for the integrated DOS reaches to the form

$$\frac{D(E)}{D_0a_0^*}=\frac{g_s}{2}\sum_{n=1}^{\infty}\sum_{i=1}^{\lambda}\left(\left|\frac{dE_n(k_z)}{dk_z}\right|_{k_z=k_{z,i}}\right)^{-1}. \tag{14}$$

3. Results and discussion

In numerical calculations, the finite-barrier confinement potential V_0 is obtained from the 60% rule ($x\leq 0.45$) of the band gap discontinuity (ΔE_g) between $Al_xGa_{1-x}As$ and GaAs in the absence of the laser radiation. The conduction-band offset is estimated according to the Miller's rule, $V_0=600\times(1.155x+0.37x^2)$ (meV) [38]. It is known that, when the concentration x of Al in the superlattice barriers is varied, transparency of the system is affected and hence the system turns smoothly from the case of strongly coupled to the weakly coupled SSL. These regimes are identified with wide minibands/narrow minigaps and narrow minibands/wide minigaps, respectively [39]. In the present study the Al concentration in the barriers is fixed at $x=0.3$ and the zero reference energy is settled at the bottom of GaAs conduction band

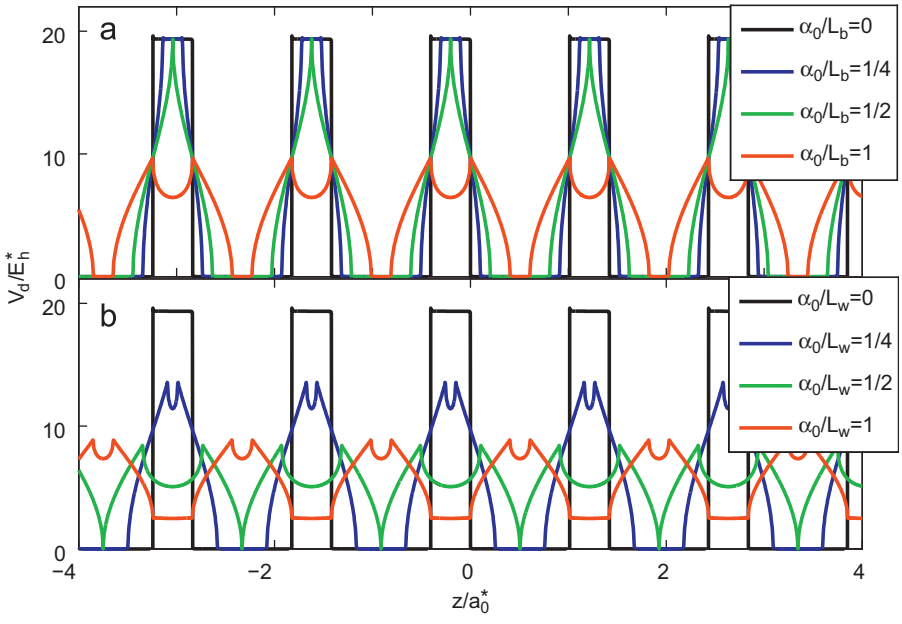

Fig. 1. Laser-dressed potential for GaAs/$Al_xGa_{1-x}As$ superlattice with $x=0.3$, $L_w=100$ Å $L_b=40$ Å for (a) $\alpha_0/L_b=0,\frac{1}{4},\frac{1}{2},1$ and (b) $\alpha_0/L_w=0,\frac{1}{4},\frac{1}{2},1$. The black straight lines state the superlattice in the absence of external EM field. (For interpretation of the references to color in this figure legend, the reader is referred to the web version of this article.)

edge which leads to the barrier height at 228 meV. The relation between the effective masses and the Al content is given as $m_w^* = 0.0665m_0$ and $m_b^* = (0.0665 + 0.083x)m_0$ where m_0 is the bare electron mass [40,41].

An array of barriers of energy V_0 in SSL gives rise to the formation of minibands for the electron motion along the superlattice axis where the minibands are separated by minigaps. The width of the minibands and the minigaps is determined by the thickness of the quantum-well and quantum-barrier layers. Electronic band structure of the system is calculated by using the series expansion method. Figs. 1(a) and (b) illustrate the laser-dressed potential for a SSL with $L_w = 100$ Å and $L_b = 40$ Å as a function of the z-position which is considered as a growth direction. The abbreviation V_d seen in the figure denotes the laser-dressed potential calculated using the Eq. (6).

It is found that ILF induces remarkable variations on the confinement potential. Fig. 1(a) illustrates the variation of the laser-dressed potential for different values of α_0 corresponding to a field-free (black line), $L_b/4$ (blue line), $L_b/2$ (green line) and L_b (red line). For a given α_0 between 0 and $L_b/2$ the barrier width decreases (increases) smoothly at the top (at the bottom). In the meantime, the opposite behavior takes place in the well region. Furthermore, for α_0 values which satisfy the condition $\alpha_0 \geq L_b/2$, an abrupt decrease in the effective height of the barrier and the formation of a symmetric pit in the barrier region is observed. The variation of the dressed-potential profile as a function of the laser field amplitudes defined with respect to the width of the well is seen in Fig. 1(b). When the laser field is turned on, the effective width of the well at the bottom (at the top) decreases (increases) linearly with the strength of the field and a symmetric pit in the barrier region is formed. We should note that in the case of $\alpha_0 = L_w$ the barrier region gets to be a well and the well region becomes as a barrier. The bottom of the pit is located at the center of the barrier and both the top and the bottom tends to 0 in the large-α_0 limit. The emergency of role-exchange between the well and the barrier, opens the possibility of creating controllable resonant states located in the material.

For a more comprehensive survey, in Fig. 2 We give a picture of the laser-dressed potential in a chromatic scale, where lighter regions are higher parts of dressed-potential. This plot emphasizes more clearly the dramatic variation of the dressed potential profile.

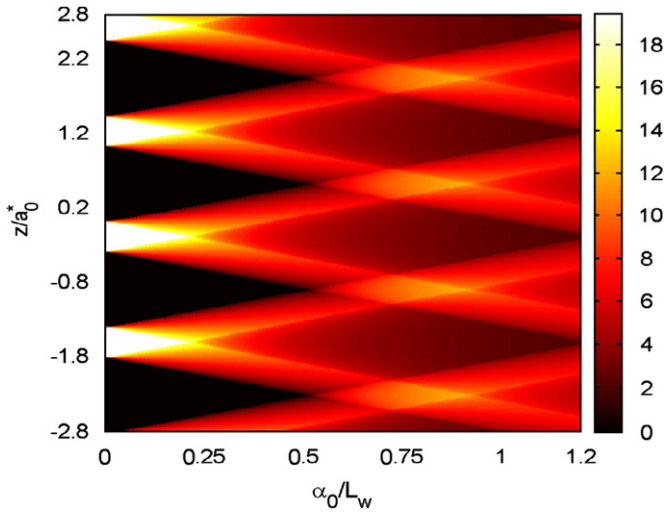

Fig. 2. Laser-dressed potential in a chromatic scale with $L_w = 100$ Å and $L_b = 40$ Å. Colorbar indicates the height of the potential. (For interpretation of the references to color in this figure legend, the reader is referred to the web version of this article.)

Next, we investigated the changes induced on the energy bands and the electron DOS. The variation of the first two bands with respect to the laser-dressing parameter is presented in Fig. 3. In the absence of a laser field the ground state miniband is found to be located between $2.77E_h^*$ and $3.07E_h^*$ above the bottom of the well and the first excited state miniband to be located at $10.13E_h^* - 11.94E_h^*$. Switching α_0 to $L_w/2$ shifts the first miniband to the energies between $5.43E_h^*$ and $7.42E_h^*$ whereas the second miniband lies in the range $7.83E_h^* - 13.08E_h^*$. The energy shifts obtained with the increase in dressing-parameter can be understood in the way that an effective well width is getting to be smaller than L_w. As a result, electronic band structure, in the point of band widths and minigaps, shows a significant dependence on the laser-dressing parameter.

One may notice that for a given α_0 between 0 and $L_w/2$ monotonic increase in the energy boundaries of the first miniband is observed whereas as α_0 increases toward L_w decrease in the energies is observed. Accordingly, the width of the first miniband increases with α_0 in the $\alpha_0 < L_w/2$ region, then the width reaches its maximum at a certain α_0-value and for further α_0-values, it begins to decrease. This non-monotonous behavior can be attributed to the oscillations of J_0-zero order Bessel functions. Larger period in space (140 Å) implies that the allowed energy minibands are very narrow [21]. Laser field causes to the change of the miniband structure, that provides a new degree of freedom in optical systems in respect of interband and intraband transitions. By considering the change of the electronic structure of the SSL in the presence of the ILF, we can say that this feature can be taken as the basis for the control of population inversion in a SSL laser operation in the optical pumping lasing scheme, in which the miniband numbers and miniband widths are taken into account for the enhancement of the rate of the population inversion [29].

The changes in the DOS calculated numerically for different values of α_0 with respect to the usual profile are depicted in Fig. 4.

It is clear from this figure that the strength of the laser-driven DOS reduces with the ILF and the general behavior of the DOS curve is consistent with that of the energy bands curves in the Fig. 3. Reduction in the DOS due to ILF enhances with the laser intensity monotonically, and it suggests an interesting tuning mechanism. The energy shifts obtained for an ILF can be extracted from the Fig. 4 by comparing the distances between each vertical line corresponding to discontinuity at $E = E_n$ and its respective

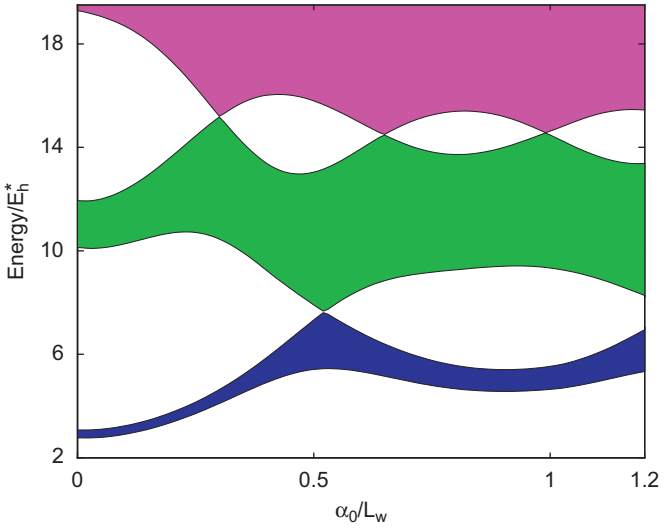

Fig. 3. The lowest and first excited bands of quasienergy for the SSL of period 140 Å, plotted vs the laser-dressing parameter.

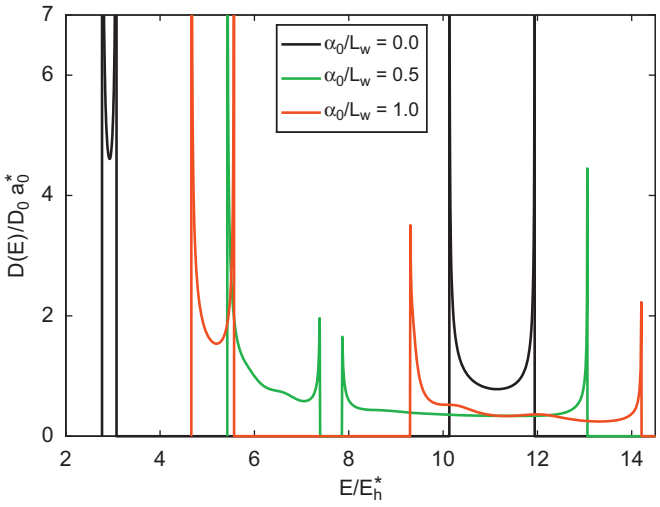

Fig. 4. The density of electron states in a GaAs/$Al_xGa_{1-x}As$ superlattice with $x=0.3$, $L_w=100$ Å and $L_b=40$ Å illuminated by an intense laser field. The black line is for the DOS in the absence of external field.

vertical black line, which refers to the state in the absence of external field. It should be noted that the variations of the band width due to the ILF can be modulated by the well width.

4. Conclusion

In summary, we have theoretically investigated the influence of an intense, high-frequency, non-resonant laser field on the electronic band structure of GaAs/$Al_xGa_{1-x}As$ semiconductor. A closed-form expression for the dressed potential of a semiconductor superlattice is derived. For the laser fields with different α_0, the dramatic variation of the formed potential in the well and barrier region is predicted. Also we conclude that the DOS decreases with strength of the ILF. The possibility of the creation of resonant states, with a good control of the energy differences is pointed out. Therefore, our results can be useful for the design of new optoelectronic devices.

Acknowledgments

We gratefully acknowledge the financial support from TUBITAK (COST) (Grant No. 109T650). CAD is grateful to the Colombian Agencies CODI-Universidad de Antioquia (Estrategia de Sostenibilidad Grupo de Materia Condensada-UdeA, 2011-2012), Facultad de Ciencias Exactas y Naturales-Universidad de Antioquia (CAD-exclusive dedication project 2011–2012), and "El Patrimonio Autónomo Fondo Nacional de Financiamiento para la Ciencia, la Tecnología y la Innovación Francisco José de Caldas" Contract RC - No. 275-2011.

References

[1] M. Santhi, A. John Peter, Physica E 42 (2010) 1643.
[2] M. Asada, Y. Miyamoto, Y. Suematsu, IEEE J. Quant. Electron. 22 (1986) 1915.
[3] P. Harrison, Quantum Wells, Wires and Dots, John Wiley and Sons, 2000.
[4] J. Silva-Valencia, N. Porras-Montenegro, Phys. Rev. B. 58 (1998) 2094.
[5] Y. Mizumoto, Y. Kayanuma, A. Srivastava, J. Kono, A.H. Chin, Phys. Rev. B 74 (2006) 045216/1.
[6] B.G. Enders, F.M.S. Lima, O.A.C. Nunes, A.L.A. Fonseca, D.A. Agrello, F. Qu, E.F. Da Silva, V.N. Freire, Phys. Rev. B 70 (2004) 035307/1.
[7] F. Ungan, U. Yesilgul, S. Sakiroglu, E. Kasapoglu, H. Sari, I. Sokmen, Phys. Lett. A 374 (2010) 2980.
[8] C.A. Duque, E. Kasapoglu, S. Sakiroglu, H. Sari, I. Sokmen, Appl. Surf. Sci. 256 (2010) 7406.
[9] C.A. Duque, E. Kasapoglu, S. Sakiroglu, H. Sari, I. Sokmen, Appl. Surf. Sci. 257 (2011) 2313.
[10] O.O.D. Neto, F. Qu, Superlattices and Microstructures 35 (2004) 1.
[11] E. Niculescu, A. Iorga, A. Radu, U. P. B. Sci. Bull. Ser. A 70 (2008) 63.
[12] D. Piester, P. Bönsch, T. Schrimpf, H.-H. Wehmann, A. Schlachetzki, IEEE J. Quant. Electron. 6 (2000) 522.
[13] L.E. Oliveira, A. Latgé, H.S. Brandi, Phys. Stat. Sol. (a) 190 (2002) 667.
[14] G. Bastard, Phys. Rev. B 24 (1981) 5693.
[15] L. Esaki, IEEE J. Quant. Electron. 22 (1986) 1611.
[16] J.H. Luscombe, R. Aggarwal, M.A. Reed, W.R. Frensley, M. Luban, Phys. Rev. B 44 (1991) 5873.
[17] H.S. Brandi, A. Latgé, L.E. Oliveira, Phys. Rev. B 64 (2001) 035323/1.
[18] J.-Y. Yan, R.-B. Liu, B.-f. Zhu, N. J. Phys. 11 (2009) 083004/1.
[19] C. Rodriguez-Castellanos, M.T. Pérez-Maldonado, Superlattices Microstruct. 27 (2000) 15.
[20] S. Winnerl, E. Schomburg, J. Grenzer, H.J. Regl, A.A. Ignatov, K.F. Renk, D.P. Pavelev, Y. Koschurinov, B. Melzer, V. Ustinov, S. Ivanov, S. Schaposchnikov, P.S. Kopev, Superlattices Microstruct. 21 (1997) 91.
[21] M. Holthaus, Phys. Rev. Lett. 69 (1992) 351.
[22] M. Holthaus, D. Hone, Phys. Rev. B 47 (1993) 6499.
[23] A. Radu, E. Niculescu, M. Cristea, J. Optoelectron. Adv. Mater. 10 (2008) 2555.
[24] F. Ungan, E. Kasapoglu, C.A. Duque, U. Yesilgul, S. Sakiroglu, I. Sokmen, Eur. Phys. J. B 80 (2011) 89.
[25] E. Kasapoglu, C.A. Duque, S. Sakiroglu, H. Sari, I. Sokmen, Physica E 43 (2011) 1427.
[26] F. Szmulowicz, Eur. J. Phys. 18 (1997) 392.
[27] L.-J. He, X.-K. Cheng, H. Li, J. Zhang, J.-M. Zhou, Q. Huang, Appl. Surf. Sci. 252 (2006) 5868.
[28] Q. Fanyao, A.L.A. Fonseca, O.A.C. Nunes, Phys. Stat. Sol. (b) 197 (1996) 349.
[29] F.M.S. Lima, M.A. Amato, O.A.C. Nunes, A.L.A. Fonseca, B.G. Enders, E.F. da Silva, J. Appl. Phys. 105 (2009) 123111/1.
[30] H. Kramers, Collected Scientific Papers, North-Holland, Amsterdam, 1956.
[31] F.M.S. Lima, O.A.C. Nunes, M.A. Amato, A.L.A. Fonseca, E.F. da Silva, J. Appl. Phys. 103 (2008) 113112/1.
[32] M. Gavrila, J.Z. Kaminski, Phys. Rev. Lett. 52 (1984) 613.
[33] M. Gavrila, Atoms in intense laser fields, in: M. Gavrila (Ed.), Advances in Atomic, Molecular and Optical Physics, Academic Press, 1992.
[34] Q. Fanyao, A.L.A. Fonseca, O.A.C. Nunes, Superlattices Microstruct. 23 (1998) 1005.
[35] O.A.C. Nunes, A.L.A. Fonseca, F.M.S. Lima, D.A. Agrello, Solid State Commun. 122 (2002) 425.
[36] G.B. Arfken, H.J. Weber, Mathematical Methods for Physicists, sixth ed., Elsevier Academic Press, 2005.
[37] E.C. Niculescu, L.M. Burileanu, Eur. Phys. J. B 74 (2010) 117.
[38] S.L. Chuang, Physics of Optoelectronic Devices, Wiley, New York, 1995.
[39] M. Steslicka, R. Kucharczyk, A. Akjouj, B. Djafari-Rouhani, L. Dobrzynski, S.G. Davison, Surf. Sci. Rep. 47 (2002) 93.
[40] W.L. Bloss, Phys. Rev. B 44 (1991) 8035.
[41] L.E. Oliveira, R. Pérez-Alvarez, Phys. Rev. B 40 (1989) 10460.